Journal of Geoscience and Environment Protection, 2026, 14(4), 300-313
https://www.scirp.org/journal/gep
ISSN Online: 2327-4344
ISSN Print: 2327-4336

Multi-Scale Spatiotemporal Characteristics of Near-Surface Wind Fields in Xinjiang, China

Hongliang Rong[1], Jing Zhang[2,3*], Shanshan Chen[4], Peng Fan[2,3], Xuzhi Zhu[2,3], Hui Qiao[2,3]

[1]Xinjiang Transportation Investment Construction Management Co., Ltd., Urumqi, China
[2]Xinjiang Transportation Science Research Institute Co., Ltd., Urumqi, China
[3]Key Laboratory of Highway Engineering Technology and Transportation Industry in Arid Desert Region, Urumqi, China
[4]Nanjing Lishui District Meteorological Bureau, Nanjing, China
Email: *346519500@qq.com

How to cite this paper: Rong, H. L., Zhang, J., Chen, S. S., Fan, P., Zhu, X. Z., & Qiao, H. (2026). Multi-Scale Spatiotemporal Characteristics of Near-Surface Wind Fields in Xinjiang, China. *Journal of Geoscience and Environment Protection, 14,* 300-313.
https://doi.org/10.4236/gep.2026.144016

Received: March 10, 2026
Accepted: April 25, 2026
Published: April 28, 2026

Abstract

Xinjiang, located in the arid and semi-arid region of northwestern China, is characterized by complex terrain and strong near-surface winds that play a crucial role in dust emission, atmospheric dispersion, wind energy utilization, and transportation safety. However, a comprehensive understanding of wind variability across different temporal scales remains limited. In this study, empirical orthogonal function (EOF) analysis is applied to near-surface wind vector fields and total wind speed over Xinjiang during 1995-2024 at sub-daily (hourly), daily, and annual time scales. The leading EOF modes and their corresponding principal components are analyzed to reveal dominant spatial patterns, temporal evolution, and associated physical interpretations. Results indicate a clear scale dependence of wind variability: hourly variability is dominated by diurnal thermal forcing and terrain-induced circulations, daily variability reflects seasonal and synoptic-scale modulation, and annual variability highlights interannual to decadal climate influences. Differences between wind vector and wind speed EOFs further emphasize the importance of directional variability in shaping regional wind dynamics. These findings provide a multi-scale perspective on wind field variability over Xinjiang and offer scientific support for wind-related climate assessment and applied meteorological services in arid regions.

Keywords

Multi-Scale, Spatiotemporal Characteristics, Near-Surface Wind, Xinjiang

1. Introduction

Near-surface winds are a fundamental component of the atmospheric system,

governing momentum exchange, turbulent mixing, and transport of heat, moisture, and aerosols within the atmospheric boundary layer. In arid and semi-arid environments, wind variability is particularly consequential because strong winds regulate wind erosion, dust emission, and sand transport, thereby affecting air quality, ecosystem stability, and human activities (Shao, 2008; Wang et al., 2022). These wind-driven processes are tightly coupled with boundary-layer dynamics and land-surface conditions, making both short-term variability and long-term changes in surface winds important for climate assessment and hazard mitigation (Lyu et al., 2022).

Xinjiang, located in northwestern China, is a typical basin-mountain system embedded in the midlatitude westerly circulation, featuring the Junggar Basin, Tarim Basin, and the Tianshan Mountains (Zhu et al., 2022). The interaction between large-scale flow and complex topography can produce strong spatial heterogeneity in wind speed and direction, including mountain-valley winds, terrain channeling, and basin-scale circulations (Whiteman, 2000). Recent regional studies further document the pronounced heterogeneity of wind speed over Xinjiang and its close association with topographic gradients and mountain-slope acceleration, emphasizing that Xinjiang is a key natural laboratory for understanding terrain-circulation coupling in arid regions.

Beyond regional characteristics, observed near-surface wind speed has experienced substantial multi-decadal variability over many land areas. A broad decline in surface wind speed (atmospheric stilling) has been documented across the Northern Hemisphere, with evidence that increasing surface roughness contributes to the slowdown in many regions. At the China scale, multiple studies have identified a weakening of surface winds during the late 20th century followed by partial recovery in recent decades, with strong spatial and seasonal dependence. For example, analyses combining multiple datasets show a stilling-recovery transition over China during 1960-2017, while other work highlights coherent (but height-dependent) trends between surface and upper-air winds, which is crucial for interpreting the mechanisms behind surface wind changes. Centennial-scale reanalysis-based assessment also indicates distinct periods in near-surface wind variations over China. More recent studies further suggest that stilling may have ended around the mid-2010s with notable regional differences (including signals over western Xinjiang).

Wind variability is inherently scale dependent. At sub-daily scales, near-surface winds are strongly modulated by diurnal thermal forcing and boundary-layer turbulence, generating mountain-valley and slope wind systems in complex terrain (Whiteman, 2000; Stull, 2012). At synoptic and seasonal scales, variability is shaped by pressure-gradient forcing and the evolution of large-scale circulation systems. At interannual to decadal scales, persistent changes in circulation regimes and jets can modulate regional wind climates. Understanding Xinjiang winds therefore requires a multi-scale framework that can isolate dominant spatiotemporal structures across hourly, daily, and annual time scales.

Despite the above advances, systematic multi-timescale EOF analyses of Xinjiang near-surface winds that explicitly compare wind vector fields and wind speed remain limited. This gap is important because wind direction variability can encode circulation regime transitions that are not apparent in scalar wind speed alone, while wind speed EOFs can highlight intensity corridors relevant to dust emission and wind energy applications.

The present study addresses these issues by applying EOF analysis to near-surface wind vectors and total wind speed over Xinjiang during 1995-2024 at hourly, daily, and annual time scales. The objectives are to 1) identify dominant spatial patterns of near-surface wind variability across time scales, 2) quantify and compare the temporal behaviors of leading modes, and 3) clarify the complementary information captured by vector-based and scalar-based EOFs. The resulting multi-scale depiction provides a physical basis for understanding wind-related climate variability and for supporting wind-sensitive applications in Xinjiang and other arid regions.

2. Data and Methodology

2.1. Data

The near-surface wind data used in this study are derived from the ERA5 reanalysis produced by the European Centre for Medium-Range Weather Forecasts (ECMWF). ERA5 is the fifth-generation global atmospheric reanalysis and provides a dynamically consistent representation of the atmospheric state based on advanced data assimilation of in situ and satellite observations (Hersbach et al., 2020). In this study, the 10-m zonal wind and meridional wind components are extracted at an hourly temporal resolution and a spatial resolution of $0.25^\circ \times 0.25^\circ$ for the Xinjiang region (73˚E-96.5˚E, 34˚N-49.5˚N) during 1995-2024 (UTC). No additional regridding is performed, and a geographic mask is applied to retain only grid points within the study domain. The total wind speed is computed based on the hourly zonal wind and meridional wind components.

2.2. Methodology

Empirical orthogonal function (EOF) analysis is a widely used statistical method for identifying dominant modes of variability in spatiotemporal datasets by decomposing the covariance structure of the data into orthogonal spatial patterns and their corresponding temporal coefficients (Lorenz, 1956; North et al., 1982; Monahan et al., 2009; Fan et al., 2022). In this study, EOF analysis is applied to near-surface wind fields over Xinjiang to extract the leading modes of variability at multiple temporal scales.

Prior to the EOF decomposition, wind fields at each temporal scale (hourly, daily, and annual) are converted into anomaly fields by removing the corresponding long-term climatological mean. More specifically, for the hourly EOF, the sample dimension corresponds to the 24 hours of the day averaged over 1995-2024. For the daily and annual EOF, the sample dimensions correspond to the calendar day of the year and the 30 individual years from 1995 to 2024, respec-

tively. Besides, to account for the decrease in grid-cell area with increasing latitude, a cosine-latitude weighting is applied to the anomaly fields. EOF analysis is then performed using the covariance matrix, allowing the dominant modes to retain the physical variance of the wind field.

In particular, for the wind vector analysis, a multivariate EOF (MV-EOF) framework is adopted to jointly analyze the zonal and meridional wind components (Wang, 1992). Specifically, for the study domain with M grid points, let x_i ($i=1,2,\cdots,M$) denote the i-th spatial grid point. The variable t ($t=1,2,\cdots,T$) represents discrete time steps, where T is the total number of temporal samples at a given timescale. The anomaly zonal and meridional wind components at grid point x_i and time t are denoted by $u'(x_i,t)$ and $v'(x_i,t)$, respectively. For convenience in matrix operations, the spatial fields are reshaped into a state vector at each time step, denoted by $\mathbf{X}(t)$, which is constructed by concatenating the wind components at all grid points:

$$\mathbf{X}(t)=\left[u_1'(t),u_2'(t),\cdots,u_M'(t),v_1'(t),v_2'(t),\cdots,v_M'(t)\right]^T$$

where $u_i'(t)=u'(x_i,t)$ and $v_i'(t)=v'(x_i,t)$. In this vector representation, the spatial index x_i is implicitly encoded in the ordering of the vector elements. The EOF decomposition yields a set of orthogonal spatial patterns (EOF modes), denoted by $\mathbf{E}_k$, and their corresponding principal components (PCs), denoted by $PC_k(t)$, where $k=1,2,\cdots,K$ indicates the mode number. At each grid point, the EOF mode provides a pair of values corresponding to the zonal and meridional components, which can be visualized together as a vector pattern, forming the spatial pattern of the mode. This approach preserves the physical consistency between wind direction and magnitude and enables the identification of coherent circulation structures (Wang et al., 2008).

For the wind speed analysis, the total wind speed is first calculated at each grid point x_i and time step t as

$$WS(x_i,t)=\sqrt{u(x_i,t)^2+v(x_i,t)^2}$$

where $u(x_i,t)$ and $v(x_i,t)$ denote the zonal and meridional wind components, respectively. Wind speed anomalies are then obtained by removing the climatological mean at each temporal scale, and EOF analysis is applied directly to the scalar wind speed field using the same covariance-based framework and latitude weighting as described above. Unlike the vector EOF, the resulting modes represent spatial variations in wind intensity only and do not explicitly contain directional information.

The temporal evolution of each EOF mode is represented by its principal component (PC), which is obtained by projecting the anomaly field onto the corresponding EOF pattern. The relative importance of each mode is quantified by the percentage of total variance explained. In this study, the leading three EOF modes are analyzed at each temporal scale, as they capture the majority of the wind variability and provide a robust representation of the dominant spatiotemporal structures.

3. Results

3.1. Sub-Daily Variability

At the hourly scale (Figure 1), the EOF analysis reveals that near-surface wind variability over Xinjiang is overwhelmingly dominated by a single leading mode. The first EOF mode explains 78.3% of the total variance, indicating a highly organized and spatially coherent circulation structure. Spatially, this mode is characterized by systematically stronger winds along mountainous regions and weaker winds over basin interiors. Such a distribution highlights the strong control of topography on near-surface winds at sub-daily time scales. The corresponding principal component (PC1) exhibits pronounced high-frequency oscillations, consistent with a strong diurnal signal. The temporal evolution suggests regular alternation between two opposite circulation phases within a day, reflecting a well-defined day-night contrast. This behavior indicates that the hourly wind field is primarily governed by periodic processes rather than episodic disturbances. The second EOF mode, accounting for 16.6% of the variance, represents a clear north-south contrast in wind direction across Xinjiang. Northern Xinjiang and southern Xinjiang exhibit opposite wind directions during daytime and nighttime, respectively, with wind speed peaking around local noon. Compared to EOF1, this mode displays greater spatial heterogeneity and reduced coherence, suggesting that it captures regional-scale adjustments superimposed on the dominant diurnal circulation. The third EOF mode explains only a small fraction of the variance but exhibits complex and localized spatial structures. Wind directions vary substantially across different subregions, and the associated PC shows a bimodal distribution in time. This mode likely reflects transient and localized processes that contribute to the residual variability of the hourly wind field. Overall, the hourly wind vector EOFs indicate a clear hierarchy of variability, with a dominant diurnal circulation pattern and progressively more localized and irregular modes.

For hourly total wind speed (Figure 2), the leading EOF mode explains 66.5% of the total variance, highlighting large-scale intensity contrasts between northern and southern Xinjiang. Wind speed variations in these two regions are largely out of phase, suggesting that they are influenced by different background flow regimes. Spatially, wind speed variability is strongest along basin margins and weaker over basin interiors, emphasizing the amplifying role of terrain on wind intensity fluctuations. The associated PC1 shows a pronounced diurnal cycle, with enhanced wind speeds during daytime and reduced values at night. Compared with wind vector EOFs, the wind speed EOFs display smoother spatial patterns, reflecting the scalar nature of wind speed and its reduced sensitivity to directional variability. The second EOF mode explains 17.8% of the variance and reveals opposite wind speed variations between basin interiors and surrounding regions. The temporal evolution exhibits a bimodal diurnal pattern, with wind speed maxima typically occurring in the afternoon. This behavior is consistent with the influence of surface heating and land-surface heterogeneity on hourly wind speed variability.

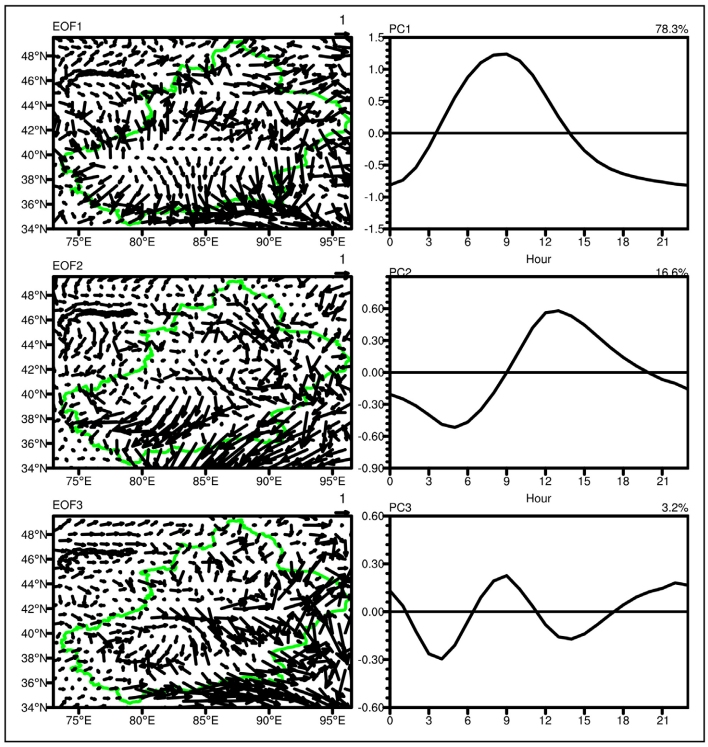

Figure 1. Hourly EOF modes of near-surface wind vectors and their corresponding time series over Xinjiang from 1995 to 2024.

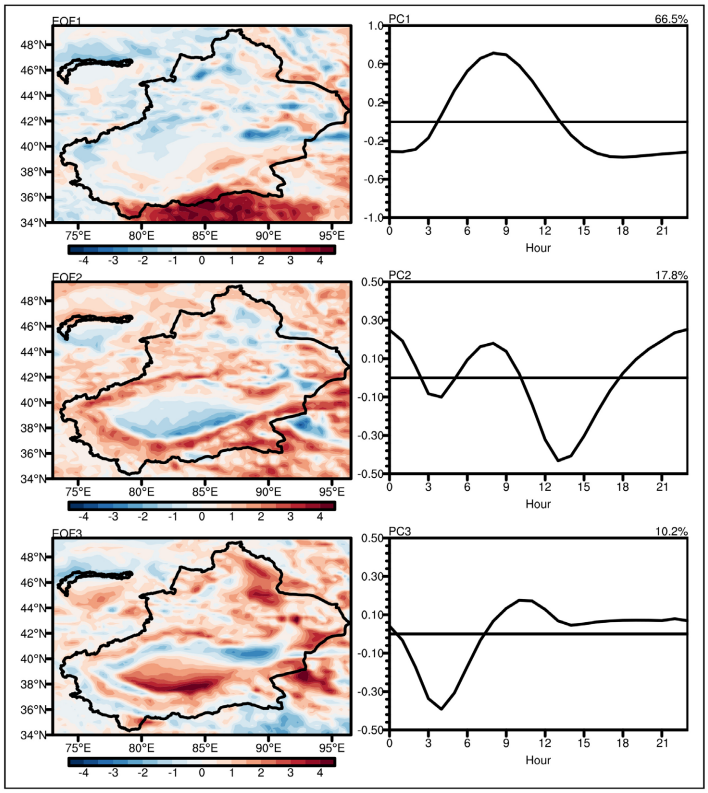

Figure 2. Hourly EOF modes of near-surface total wind speed and their corresponding time series over Xinjiang from 1995 to 2024.

3.2. Daily Variability

At the daily scale (Figure 3), the leading EOF mode of the wind vector field explains 75.9% of the variance, indicating that a single dominant circulation pattern also governs day-to-day wind variability. Spatially, this mode is characterized by a transition from northwesterly winds in northern Xinjiang to northeasterly winds in southern Xinjiang. Compared with the hourly EOF1, the spatial pattern is smoother and more regionally coherent, reflecting the suppression of high-frequency variability. The corresponding PC1 exhibits a pronounced seasonal cycle, with positive values during summer and negative values during winter. This seasonal contrast suggests that daily wind variability is influenced by the annual cycle of large-scale circulation and regional thermal conditions. The second EOF mode accounts for 6.4% of the variance and highlights enhanced wind activity over southern and eastern Xinjiang, with the strongest influence during spring. This mode might be associated with regional-scale variability that becomes more prominent during transitional seasons, when synoptic disturbances are generally more frequent. The third EOF mode reveals a distinct cyclonic circulation over the Tarim Basin. The associated PC shows a bimodal seasonal distribution, suggesting that this circulation pattern tends to intensify during specific seasons rather than persisting throughout the year.

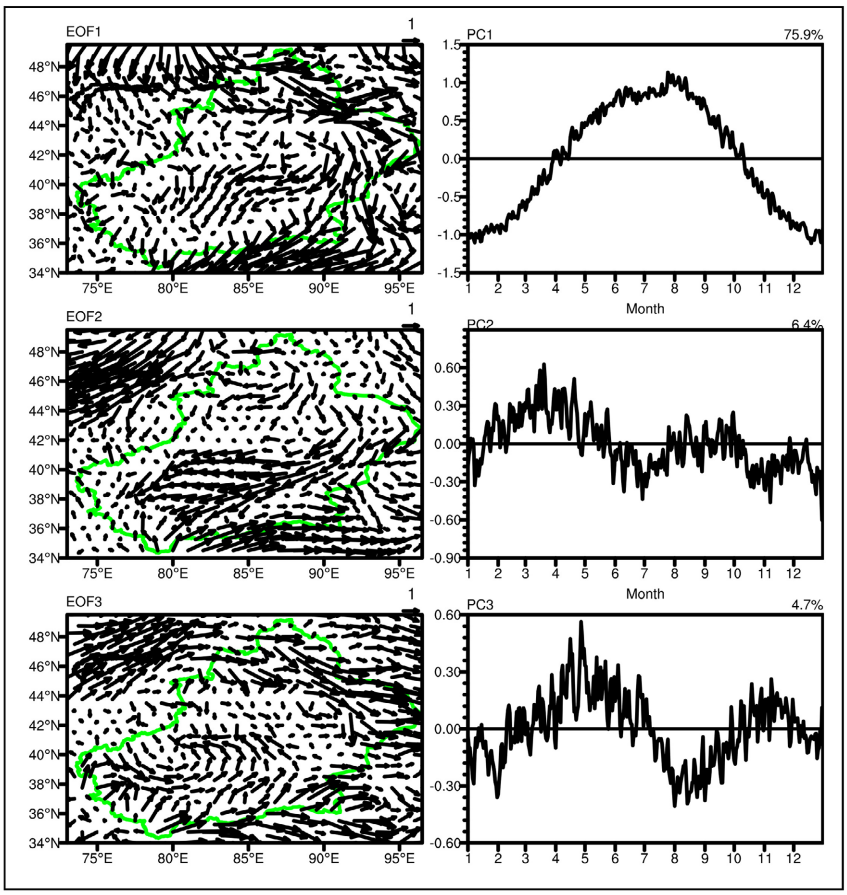

Figure 3. Daily EOF modes of near-surface wind vectors and their corresponding time series over Xinjiang averaged for the period 1995-2024.

The first EOF mode of daily wind speed explains 60.2% of the total variance and exhibits strong wind speed variability within basin regions, contrasted with weaker and oppositely phased variability over mountainous areas (Figure 4). Basin wind speeds are systematically higher during the warm season and lower during the cold season. The second EOF mode, accounting for 10.5% of the variance, shows a clear north-south contrast in wind speed variability. The associated PC displays a bimodal seasonal structure, indicating that wind speed anomalies in northern and southern Xinjiang peak during different seasons. The third EOF mode explains 8.5% of the variance and primarily represents wind speed variability over southern Xinjiang, especially the Tarim Basin, underscoring the regional specificity of daily wind speed fluctuations.

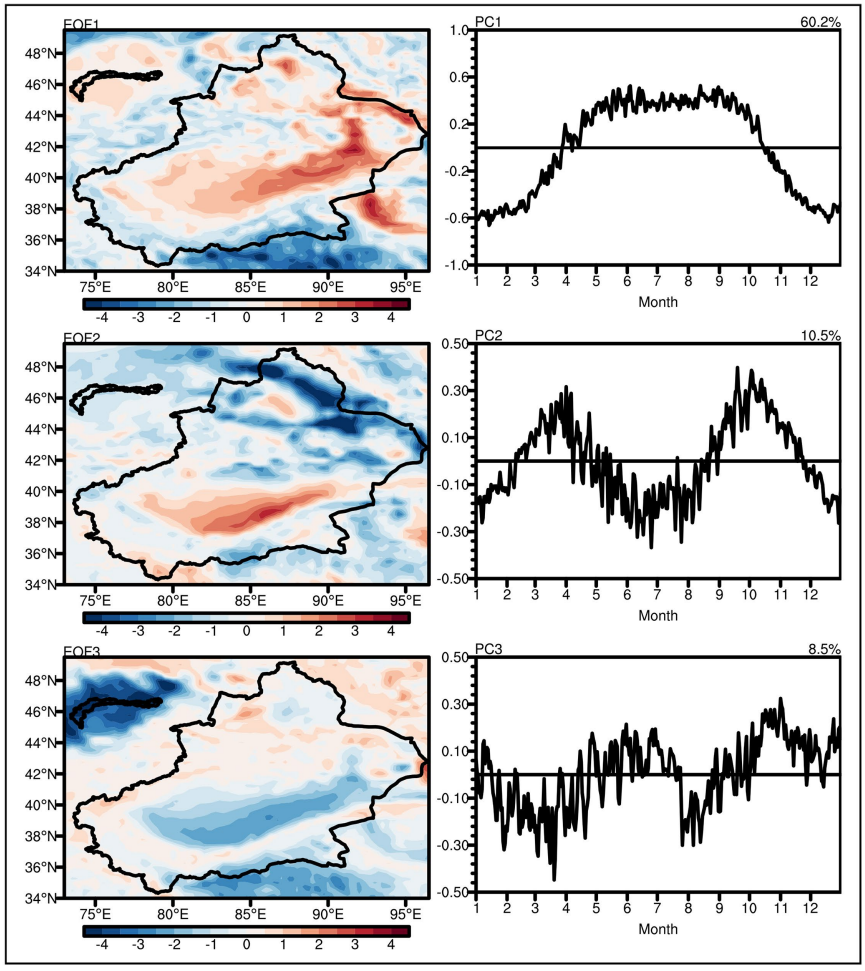

Figure 4. Daily EOF modes of near-surface total wind speed and their corresponding time series over Xinjiang averaged for the period 1995-2024.

3.3. Interannual Variability

At the annual scale (Figure 5), the dominance of a single mode weakens considerably. The first EOF mode explains 31.4% of the variance and is characterized by easterly winds over most of Xinjiang, with the most pronounced variability over

the Tarim Basin. The corresponding PC exhibits marked interannual variability superimposed on low-frequency fluctuations, indicating that long-term modulation might play an important role at this scale. It should be noted that the annual PCs are discussed here mainly in terms of interannual and low-frequency variability, and no formal trend attribution is attempted in this study. The second EOF mode explains 12.9% of the variance and features an easterly-dominated circulation with a prominent high-wind belt near the Tianshan Mountains. The third EOF mode explains 9.1% of the variance and displays contrasting circulation regimes across Xinjiang: westerlies in northern Xinjiang, easterlies in eastern Xinjiang, and a cyclonic circulation in southern Xinjiang. The associated PC shows interannual fluctuations with a decreasing tendency, indicating a possible weakening of this circulation pattern.

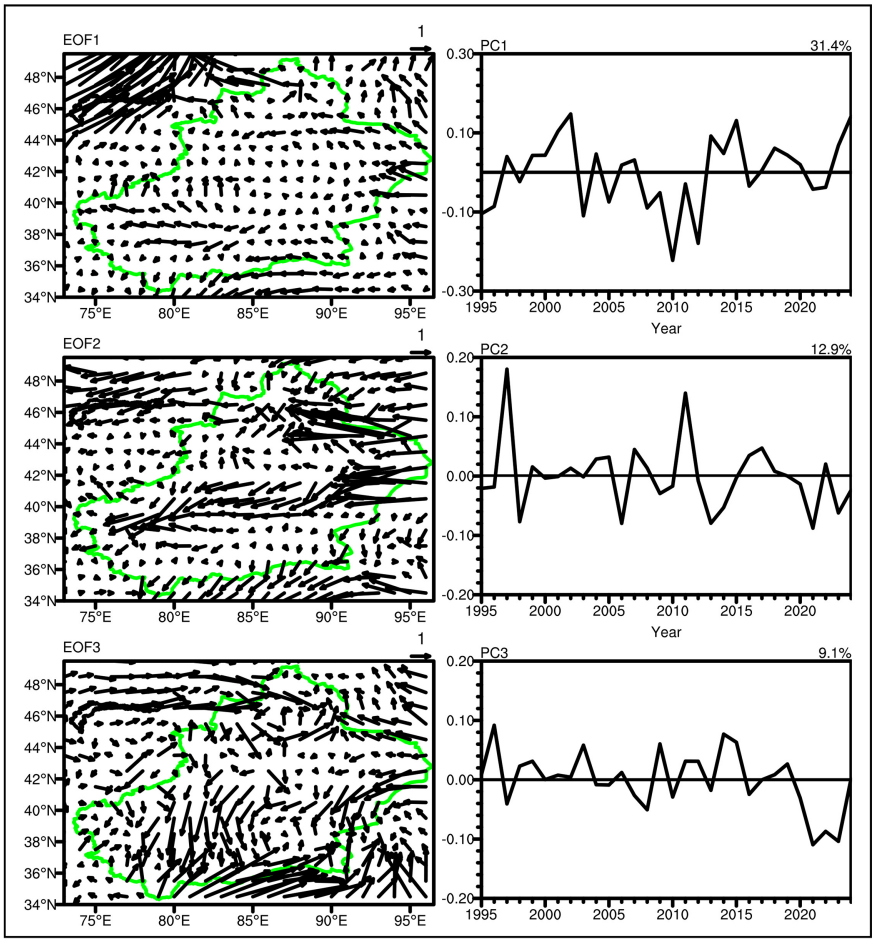

Figure 5. Interannual EOF modes of near-surface wind vectors and their corresponding time series over Xinjiang from 1995 to 2024.

The first EOF mode of annual wind speed explains 34.8% of the variance and highlights the Tarim Basin as the region with the strongest wind speed variability, which is out of phase with the rest of Xinjiang (Figure 6). The PC shows pronounced interannual variability together with evident low-frequency fluctuations.

The second EOF mode accounts for 13.6% of the variance and reveals opposing wind speed variations between basin and mountainous regions, with the strongest signals over southern and eastern Xinjiang. The third EOF mode explains 10.4% of the variance and represents a coherent wind speed variation across Xinjiang, with more pronounced changes in southern and eastern regions. The corresponding PC exhibits interannual variability with a decreasing tendency.

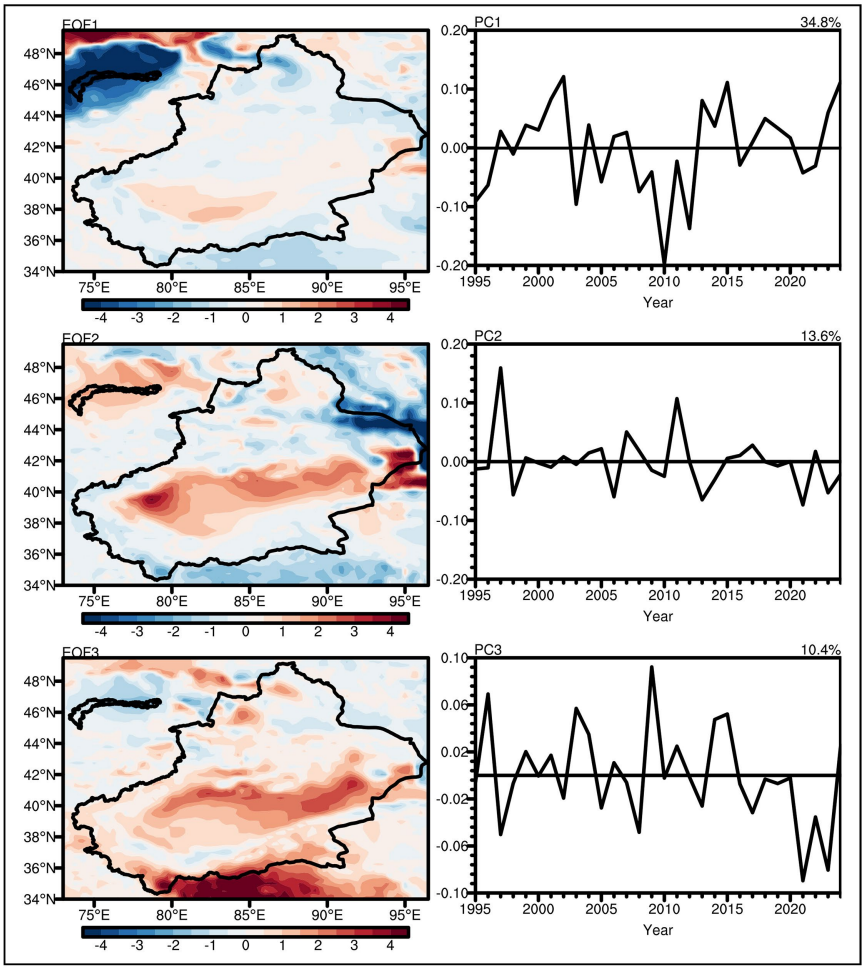

Figure 6. Interannual EOF modes of near-surface total wind speed and their corresponding time series over Xinjiang from 1995 to 2024.

3.4. Cross-Scale Comparison of Wind Variability

A comparison across temporal scales reveals a systematic transition in the nature of wind variability over Xinjiang. At the hourly scale, wind variability is dominated by highly regular and spatially coherent diurnal processes. At the daily scale, seasonal modulation becomes more prominent, while synoptic-scale influences introduce regional contrasts. At the annual scale, variability is more evenly distributed among multiple EOF modes, reflecting the increasing importance of interannual and decadal climate modulation.

Furthermore, wind vector EOFs consistently emphasize directional changes

and circulation structures, whereas wind speed EOFs highlight intensity contrasts and regional amplitude differences. The complementary nature of these two representations provides a more complete depiction of near-surface wind variability over Xinjiang.

4. Discussion

In summary, this study demonstrates that near-surface wind variability over Xinjiang is governed by a hierarchy of processes operating across temporal scales, ranging from diurnal boundary-layer dynamics to synoptic modulation and large-scale circulation variability (Rotach et al., 2022). The Asian westerly jet and associated midlatitude dynamics likely play an important role in shaping daily to interannual wind variability, while complex terrain amplifies and redistributes these influences at regional and local scales (Lei et al., 2021). These findings advance understanding of wind dynamics in arid and semi-arid regions and provide a robust physical basis for future studies on dust activity, wind energy resources, and climate-related wind hazards over Xinjiang and similar environments.

5. Conclusion

The study provides a comprehensive multi-timescale assessment of near-surface wind variability over Xinjiang using empirical orthogonal function (EOF) analysis applied to wind vector fields and total wind speed at hourly, daily, and annual resolutions during 1995-2024. The results demonstrate a pronounced scale dependence of wind variability, with distinct dominant modes emerging at different temporal scales and allowing physically plausible interpretations of their associated drivers.

At the hourly scale, near-surface wind variability is overwhelmingly dominated by a coherent leading mode that is likely associated with diurnal thermal forcing and boundary-layer processes over complex terrain (Whiteman, 2000). The strong spatial correspondence between wind anomalies and topographic features suggests the important role of the basin-mountain system in modulating wind direction and intensity. Such diurnal wind systems are a well-documented feature of mountainous regions, arising from differential heating and cooling between mountain slopes and basin interiors and from the associated buoyancy-driven pressure gradients (Zardi & Whiteman, 2013). In addition, the daytime evolution of local wind systems in mountain valleys is closely tied to boundary-layer development and thermally induced circulations (De Wekker & Kossmann, 2015; Fernando et al., 2015). Therefore, the dominance of a single EOF mode at this scale suggests that sub-daily wind variability over Xinjiang is strongly influenced by periodic processes, and the leading hourly EOF mode can be interpreted as being physically consistent with thermally driven local circulations, although this mechanism is not directly diagnosed in the present study.

At the daily scale, the leading EOF modes reveal a transition toward stronger seasonal and synoptic modulation. The primary wind vector mode exhibits a clear

seasonal phase reversal, which is consistent with the annual cycle of large-scale circulation and thermal contrast over midlatitude Asia (Wallace & Hobbs, 2006; Wei et al., 2017). Secondary modes emphasize regional contrasts, particularly over southern and eastern Xinjiang, suggesting enhanced sensitivity to synoptic disturbances during transition seasons, when transient eddy activity and circulation variability are generally more pronounced (Ren et al., 2010; Zhao et al., 2014). Taken together, these results suggest that daily wind variability may be influenced by both background circulation and regional thermal forcing, thereby bridging the gap between diurnal boundary-layer dynamics and longer-term climate variability.

At the annual scale, the variance explained by individual EOF modes decreases substantially, indicating a more complex structure of interannual and low-frequency variability. The leading annual modes highlight persistent wind anomalies over the Tarim Basin and surrounding regions, accompanied by pronounced interannual fluctuations and low-frequency variations. This behavior is consistent with previous studies showing that near-surface winds can exhibit marked low-frequency variability associated with changes in atmospheric circulation and land-surface conditions (Zhang & Wang, 2020). In the context of China, recent work has further shown that long-term surface wind variations reflect a combination of stilling, partial recovery, and circulation-related modulation (Deng et al., 2021).

The comparison between wind vector and wind speed EOFs underscores the complementary nature of these two representations. Wind vector EOFs effectively capture directional variability and circulation structures associated with regime shifts, while wind speed EOFs emphasize intensity contrasts and regional amplitude differences that are particularly relevant for dust emission, wind energy assessment, and wind-related hazards. The combined use of vector and scalar wind fields therefore provides a more complete depiction of near-surface wind variability than either representation alone.

Acknowledgements

The authors acknowledge the support by the Project of Xinjiang Transportation Investment and Construction Management Co. Ltd. (XJJTZKX-FWCG-202411-0738 and XJJTZKX-FWCG-202401-0043).

Conflicts of Interest

The authors declare no conflicts of interest regarding the publication of this paper.

References

De Wekker, S. F. J., & Kossmann, M. (2015). Convective Boundary Layer Heights over Mountainous Terrain—A Review of Concepts. *Frontiers in Earth Science, 3,* Article 77. https://doi.org/10.3389/feart.2015.00077

Deng, K., Azorin-Molina, C., Minola, L., Zhang, G., & Chen, D. (2021). Global Near-Surface Wind Speed Changes over the Last Decades Revealed by Reanalyses and CMIP6 Model Simulations. *Journal of Climate, 34,* 2219-2234.

https://doi.org/10.1175/jcli-d-20-0310.1

Fan, Y., Li, J., Zhu, S., Li, H., & Zhou, B. (2022). Trends and Variabilities of Precipitation and Temperature Extremes over Southeast Asia during 1981-2017. *Meteorology and Atmospheric Physics, 134,* Article No. 78. https://doi.org/10.1007/s00703-022-00913-6

Fernando, H. J. S., Pardyjak, E. R., Di Sabatino, S. et al. (2015). The MATERHORN: Unraveling the Intricacies of Mountain Weather. *Bulletin of the American Meteorological Society, 96,* 1945-1967.

Hersbach, H., Bell, B., Berrisford, P. et al. (2020). The ERA5 Global Reanalysis. *Quarterly Journal of the Royal Meteorological Society, 146,* 1999-2049.

Lei, J., Shi, Z., Xie, X., Sha, Y., Li, X., Liu, X. et al. (2021). Seasonal Variation of the Westerly Jet over Asia in the Last Glacial Maximum: Role of the Tibetan Plateau Heating. *Journal of Climate, 34,* 2723-2740. https://doi.org/10.1175/jcli-d-20-0438.1

Lorenz, E. N. (1956). *Empirical Orthogonal Functions and Statistical Weather Prediction*. Massachusetts Institute of Technology, Department of Meteorology.

Lyu, Y., Zhi, X., Wu, H., Zhou, H., Kong, D., Zhu, S. et al. (2022). Analyses on the Multimodel Wind Forecasts and Error Decompositions over North China. *Atmosphere, 13,* Article 1652. https://doi.org/10.3390/atmos13101652

Monahan, A. H., Fyfe, J. C., Ambaum, M. H. P., Stephenson, D. B., & North, G. R. (2009). Empirical Orthogonal Functions: The Medium Is the Message. *Journal of Climate, 22,* 6501-6514. https://doi.org/10.1175/2009jcli3062.1

North, G. R., Bell, T. L., Cahalan, R. F., & Moeng, F. J. (1982). Sampling Errors in the Estimation of Empirical Orthogonal Functions. *Monthly Weather Review, 110,* 699-706. https://doi.org/10.1175/1520-0493(1982)110<0699:seiteo>2.0.co;2

Ren, X., Yang, X., & Chu, C. (2010). Seasonal Variations of the Synoptic-Scale Transient Eddy Activity and Polar Front Jet over East Asia. *Journal of Climate, 23,* 3222-3233. https://doi.org/10.1175/2009jcli3225.1

Rotach, M. W., Serafin, S., Ward, H. C., Arpagaus, M., Colfescu, I., Cuxart, J. et al. (2022). A Collaborative Effort to Better Understand, Measure, and Model Atmospheric Exchange Processes over Mountains. *Bulletin of the American Meteorological Society, 103,* E1282-E1295. https://doi.org/10.1175/bams-d-21-0232.1

Shao, Y. (2008). *Physics and Modelling of Wind Erosion*. Springer.

Stull, R. B. (2012). *An Introduction to Boundary Layer Meteorology*. Springer.

Wallace, J. M., & Hobbs, P. V. (2006). *Atmospheric Science: An Introductory Survey*. Elsevier.

Wang, B. (1992). The Vertical Structure and Development of the ENSO Anomaly Mode during 1979-1989. *Journal of the Atmospheric Sciences, 49,* 698-712. https://doi.org/10.1175/1520-0469(1992)049<0698:tvsado>2.0.co;2

Wang, B., Wu, Z., Li, J., Liu, J., Chang, C., Ding, Y. et al. (2008). How to Measure the Strength of the East Asian Summer Monsoon. *Journal of Climate, 21,* 4449-4463. https://doi.org/10.1175/2008jcli2183.1

Wang, Y., Bai, Y., Zhi, X., Wu, K., Zhao, T., Zhou, Y. et al. (2022). Two Typical Patterns of Regional PM2.5 Transport for Heavy Air Pollution over Central China: Rapid Transit Transport and Stationary Accumulation Transport. *Frontiers in Environmental Science, 10,* Article 890514. https://doi.org/10.3389/fenvs.2022.890514

Wei, W., Zhang, R., Wen, M., & Yang, S. (2017). Relationship between the Asian Westerly Jet Stream and Summer Rainfall over Central Asia and North China: Roles of the Indian Monsoon and the South Asian High. *Journal of Climate, 30,* 537-552. https://doi.org/10.1175/jcli-d-15-0814.1

Whiteman, C. D. (2000). *Mountain Meteorology: Fundamentals and Applications*. Oxford University Press.

Zardi, D., & Whiteman, C. D. (2013). Diurnal Mountain Wind Systems. In: *Mountain Weather Research and Forecasting: Recent Progress and Current Challenges* (pp. 35-119). Springer. https://doi.org/10.1007/978-94-007-4098-3_2

Zhang, Z., & Wang, K. (2020). Stilling and Recovery of the Surface Wind Speed Based on Observation, Reanalysis, and Geostrophic Wind Theory over China from 1960 to 2017. *Journal of Climate, 33,* 3989-4008. https://doi.org/10.1175/jcli-d-19-0281.1

Zhao, Y., Wang, M., Huang, A., Li, H., Huo, W., & Yang, Q. (2014). Relationships between the West Asian Subtropical Westerly Jet and Summer Precipitation in Northern Xinjiang. *Theoretical and Applied Climatology, 116,* 403-411. https://doi.org/10.1007/s00704-013-0948-3

Zhu, Y., Zhi, X., Lyu, Y., Zhu, S., Tong, H., Mamtimin, A. et al. (2022). Forecast Calibrations of Surface Air Temperature over Xinjiang Based on U-Net Neural Network. *Frontiers in Environmental Science, 10,* Article 1011321. https://doi.org/10.3389/fenvs.2022.1011321